Nonreciprocal entanglement in cavity-magnon optomechanics

Jiaojiao Chen [1], Xiao-Gang Fan,[1] Wei Xiong [2,*] Dong Wang,[1] and Liu Ye[1,†]

[1]*Department of Physics and Optoelectronic Engineering, Anhui University, Anhui 230000, China*
[2]*Department of Physics, Wenzhou University, Zhejiang 325035, China*

Cavity optomechanics, a promising platform to investigate macroscopic quantum effects, has been widely used to study nonreciprocal entanglement with the Sagnac effect. Here, we propose an alternative way to realize nonreciprocal entanglement among magnons, photons, and phonons in a hybrid cavity-magnon optomechanics, where the magnon Kerr effect is used. We show that the Kerr effect gives rise to a magnon frequency shift and an additional two-magnon effect. Both of them can be tuned from positive to negative via tuning the magnetic field direction, leading to nonreciprocity. By tuning system parameters such as magnon frequency detuning or the coefficient of the two-magnon effect, bipartite and tripartite entanglements can be nonreciprocally enhanced. By further studying the defined bidirectional contrast ratio, we find that nonreciprocity in our system can be switched on and off, and can be engineered by the bath temperature. Our proposal not only provides a potential path to demonstrate nonreciprocal entanglement with the magnon Kerr effect, but also opens a direction to engineer and design diverse nonreciprocal devices in hybrid cavity-magnon optomechanics with nonlinear effects.

I. INTRODUCTION

Macroscopic quantum entanglement, as a core resource in quantum information science [1], is crucial to understand the classical-to-quantum boundary [2]. Such entanglement is generally generated in bilinear or nonlinear quantum systems. Cavity optomechanics (COM) [3], formed by photons nonlinearly coupled to phonons via radiation pressure, is a promising platform to investigate quantum effects [4–11], especially for macroscopic quantum effects theoretically [12–16] and experimentally [17–21]. Very recently, nonreciprocal entanglement in COM has attracted great interest [22,23]. This is because entanglement can be well protected (enhanced) by breaking the Lorentz reciprocity [22]. Utilizing this, various nonreciprocal devices in COM have been realized [24–31]. Previous proposals for studying nonreciprocal entanglement in COM [22,23] mainly rely on the Sagnac effect [32,33], which causes a positive or negative shift on the cavity resonance frequency, dependent on the direction of the driving field on the cavity. Apart from COM, magnons in the Kittle mode of ferromagnetic yttrium iron garnet (YIG) spheres [34–38] can also provide new insights for studying macroscopic quantum effects [39–41]. This is due to the fact that magnons have an intrinsic Kerr effect from the magnetocrystallographic anisotropy [42,43], which can also give a positive or negative frequency shift on the Kittle mode by tuning the direction of the magnetic field [44–46]. The Kerr effect has been employed to investigate various phenomena, including multistability [42–44], long-distance spin-spin interactions [47], quantum phase transitions [48,49], and

sensitive detection [50]. However, nonreciprocal entanglement has not yet been revealed with the Kerr effect.

Here, we propose how to realize nonreciprocal bi- and tripartite entanglements in a hybrid cavity-magnon optomechanics. We find that, not only all bipartite entanglements but also a genuine tripartite entanglement can be generated in the absence of the magnon Kerr effect, and the initial optomechanical entanglement can be partially transferred to the cavity-magnon and magnon-phonon subsytems. When the Kerr effect is considered, a mean magnon-number-dependent frequency shift on the magnons is produced. Similar to the Sagnac effect [32,33] on the cavity field, the Kerr-effect-induced frequency shift can be positive or negative by tuning the direction of the magnetic field. Different from the Sagnac effect, the magnon Kerr effect also gives rise to an additional two-magnon effect, which modulates the maximum values of all entanglements in our setup. As a result, both the optomechanical and magnon-phonon entanglements are reduced, but the magnon-photon and the tripartite entanglements are enhanced, compared to the case without the Kerr effect. By further tuning the aligned magnetic field along the crystallographic axis [100] or [110], one can see that all entanglements can be nonreciprocally generated. Interestingly, all entanglements except for the optomechanical entanglement can be nonreciprocally enhanced with accessible parameters. This indicates that entanglement transfer from the optomechancial entanglement to the cavity-magnon and magnon-phonon subsystems is nonreciprocal. Finally, we show that perfect nonreciprocity for all bi- and tripartite entanglements can be achieved, by studying the defined bidirectional contrast ratio. The achieved bi- and tripartite entanglements in our proposal are continuous variable (CV) entanglements, which have been widely applied to quantum transduction [51,52], quantum networking [53–58], quantum sensing [59], Bell-state

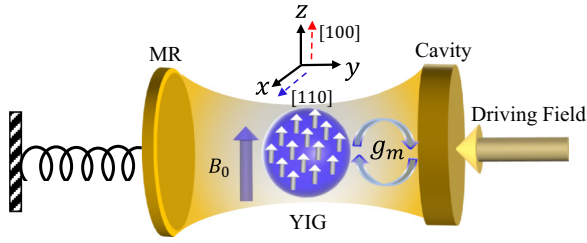*xiongweiphys@wzu.edu.cn
†yeliu@ahu.edu.cn

FIG. 1. (a) Schematic diagram of the proposed cavity-magnon optomechanical system. It consists of a driven cavity simultaneously coupled to both a Kittle mode with Kerr nonlinearity in a YIG sphere and a MR, with coupling strength g_m and g_0, respectively. The YIG sphere is placed in a static magnetic field, along the crystallographic axis [100] (see the red-arrowed line) or [110] (see the blue-arrowed line) of the YIG sphere.

test [60], quantum teleportation [61–63], microwave-optics conversion [64–67], and other CV quantum information processing [68–71]. Thus, CV entanglement can be regarded as a useful resource for CV quantum information science. Our work provides a potential way to nonreciprocally enhance and engineer quantum entanglement with the Kerr effect, and opens a promising path to realize diverse nonreciprocal devices with the magnon Kerr effect.

II. MODEL AND HAMILTONIAN

We consider a hybrid cavity-magnon optomechanical system consisting of a strongly driven cavity with frequency ω_a coupled to both a mechanical resonator (MR) with frequency ω_b and a micron-size YIG sphere supporting a Kittle mode with frequency ω_m, where the YIG sphere is positioned in a static magnetic field B_0 (see Fig. 1). The Hamiltonian of the proposed hybrid system can be written as (setting $\hbar = 1$) $H = H_{om} + H_{kerr} + H_{int} + H_d$, where the COM Hamiltonian, $H_{om} = \omega_a a^\dagger a + \frac{1}{2}\omega_b(p^2 + q^2) - g_0 a^\dagger a q$, describes the radiation pressure interaction between the cavity field and the MR. $g_0 = (\omega_a/L)\sqrt{\hbar/m\omega_b}$ is the single-photon optomechanical coupling strength, with L being the cavity length in the absence of the intracavity field and m the effective mass of the MR. The second term $H_{kerr} = \omega_m m^\dagger m + K_0(m^\dagger m)^2$ characterizes the Kerr nonlinearity of magnons in the Kittle mode, where K_0 is reversely proportional to the volume of the YIG sphere, and its sign can be tuned by varying the direction of the static magnetic field. Specifically, when the crystallographic axis [100] ([110]) is aligned along the magnetic field, $K_0 > 0$ (< 0) [44]. Experimentally, K_0 can be tuned from 0.05 to 100 nH for the diameter of the YIG sphere from 1 mm to 100 μm. Here, a ($a^\dagger$) and m ($m^\dagger$) are the annihilation (creation) operators of the cavity and Kittle modes, respectively, and q (p) is the dimensionless position (momentum) quadrature of the MR. The Hamiltonian $H_{int} = g_m(a^\dagger m + am^\dagger)$ represents the magnetic dipole coupling between the cavity and the Kittle mode with the tunable coupling strength g_m. The last term, $H_d = i\Omega_0(a^\dagger e^{-i\omega_0 t} - ae^{i\omega_0 t})$ with frequency ω_0 and Rabi frequency Ω_0, denotes the coupling between the driving field and the cavity. With the strong driving field ($\Omega_0 \gg \kappa_a, \gamma_m$), the higher-order fluctuation terms in quantum Langevin equations can be safely

neglected when each operator is rewritten as the steady-state value plus its quantum fluctuation, i.e., $O \rightarrow O_s + O$, with $O = a, m, q, p$. Then the linearized Hamiltonian of the hybrid system is given by (see the detailed derivation in the Appendix)

$$\mathcal{H} = \tilde{\Delta}_a a^\dagger a + \tilde{\Delta}_m m^\dagger m + \frac{1}{2}\omega_b(q^2 + p^2) - \frac{1}{\sqrt{2}}g_b(a + a^\dagger)q$$
$$+ g_m(a^\dagger m + am^\dagger) + \frac{1}{2}K(m^{\dagger 2} + m^2), \quad (1)$$

where $\tilde{\Delta}_a = \omega_a - \omega_0 - g_0 q_s$ is the effective cavity frequency detuning induced by the displacement q_s of the MR, and $\tilde{\Delta}_m = \Delta_m + \Delta_K$, with the magnon frequency detuning $\Delta_m = \omega_m - \omega_0$ and the magnon frequency shift $\Delta_K \equiv 2K$, is the effective magnon frequency detuning induced by the magnon Kerr effect. The defined parameter $K \equiv 2K_0 N_m$ characterizes the strength of the two-magnon effect, which can squeeze magnons [47]. As K_0 can be positive (negative), so $K > 0$ (< 0), leading to $\Delta_K > 0$ (< 0). Obviously, K can be significantly amplified by the steady-state magnon number $N_m = |m_s|^2$, which can be indirectly tuned by the strong driving field acting on the cavity, via the beam-splitter interaction between the cavity and the Kittle mode (i.e., $a^\dagger m + am^\dagger$). $g_b \equiv \sqrt{2}g_0 a_s$ is the effective linearized optomechanical coupling strength, directly tuned by the strong driving field acting on the cavity (i.e., $a_s \propto \Omega_0$). For simplicity, m_s is assumed to be real via properly choosing the phase of the driving field.

III. DYNAMICS AND ENTANGLEMENT METRIC

According to the quantum Langevin equation, the dynamics of the linearized hybrid system governed by the Hamiltonian (1) can be written as (see details in the Appendix)

$$\dot{q} = \omega_b p, \quad \dot{p} = -\omega_b q + g_b(a + a^\dagger)/\sqrt{2} - \gamma_b p + \xi,$$
$$\dot{a} = -(i\tilde{\Delta}_a + \kappa_a)a + ig_b q/\sqrt{2} - ig_m m + \sqrt{2\kappa_a}a_{in}, \quad (2)$$
$$\dot{m} = -(i\tilde{\Delta}_m + \gamma_m)m - ig_m a - iKm^\dagger + \sqrt{2\gamma_m}m_{in},$$

where a_{in}, m_{in}, and ξ are the input noise operators with zero-mean value (i.e., $\langle a_{in}\rangle = \langle m_{in}\rangle = \langle\xi\rangle = 0$). Under the Markovian approximation, two-time correlation functions of these input noise operators in the resolved sideband regime (i.e., $\omega_b \gg \gamma_b$) are given by [72] $\langle a_{in}^\dagger(t')a_{in}(t)\rangle = \bar{n}_a\delta(t - t')$, $\langle a_{in}(t)a_{in}^\dagger(t')\rangle = (\bar{n}_a + 1)\delta(t - t')$, $\langle m_{in}^\dagger(t')m_{in}(t)\rangle = \bar{n}_m\delta(t - t')$, $\langle m_{in}(t)m_{in}^\dagger(t')\rangle = (\bar{n}_m + 1)\delta(t - t')$, $\langle\xi(t)\xi(t') + \xi(t')\xi(t)\rangle/2 \simeq \gamma_b(2\bar{n}_b + 1)\delta(t - t')$, where $\bar{n}_\sigma = [\exp(\hbar\omega_\sigma/k_B T - 1)]^{-1}$ ($\sigma = a, b, m$), with k_B being the Boltzmann constant and T the bath temperature, are the mean thermal excitation number in the cavity, the Kittle mode, and the MR, respectively. In compact form, Eq. (2) can be rewritten as $\dot{u}(t) = Au(t) + f(t)$, where $u(t) = [x_a(t), y_a(t), x_m(t), y_m(t), q(t), p(t)]^T$ and $f(t) = [\sqrt{2\kappa_a}x_{in}^a(t), \sqrt{2\kappa_a}y_{in}^a(t), \sqrt{2\gamma_m}x_{in}^m(t), \sqrt{2\gamma_m}y_{in}^m(t), 0, \xi(t)]^T$ are the vectors of the system and the input noise operators, respectively, and the drift (coefficient) matrix A is (see details

in the Appendix)

$$A = \begin{pmatrix} -\kappa_a & \tilde{\Delta}_a & 0 & g_m & 0 & 0 \\ -\tilde{\Delta}_a & -\kappa_a & -g_m & 0 & g_b & 0 \\ 0 & g_m & -\gamma_m & \tilde{\Delta}_m^- & 0 & 0 \\ -g_m & 0 & -\tilde{\Delta}_m^+ & -\gamma_m & 0 & 0 \\ 0 & 0 & 0 & 0 & 0 & \omega_b \\ g_b & 0 & 0 & 0 & -\omega_b & -\gamma_b \end{pmatrix}, \quad (3)$$

where $\tilde{\Delta}_m^\pm = \tilde{\Delta}_m \pm \Delta_K/2$.

Since the input quantum noises are zero-mean quantum Gaussian noises, the quantum steady state for the fluctuations is a zero-mean CV three-mode Gaussian state, fully characterized by a 6×6 covariance matrix $\mathcal{V}_{ij} = \langle u_i(t)u_j(t') + u_j(t')u_i(t)\rangle/2$ $(i, j = 1, 2, \ldots, 6)$, where the steady-state $\mathcal{V}$ can be given by solving the Lyapunov equation

$$A\mathcal{V} + \mathcal{V}A^T = -D. \quad (4)$$

Here, $D = \mathrm{diag}[\kappa_a(2\bar{n}_a + 1), \quad \kappa_a(2\bar{n}_a + 1), \gamma_m(2\bar{n}_m + 1),$ $\gamma_m(2\bar{n}_m + 1), 0, \gamma_b(2\bar{n}_b + 1)]$ is defined by $\langle n_i(t)n_j(t') + n_j(t')n_i(t)\rangle/2 = D_{ij}\delta(t - t')$. To investigate bipartite and tripartite entanglement of the proposed system, the logarithmic negativity E_N [73,74] and the residual contangle R_τ [75] are employed, respectively. A *bona fide* quantification of tripartite entanglement is given by the *minimum* residual contangle [75], $\mathcal{R}_\tau^{\min} \equiv \min[\mathcal{R}_\tau^{m|ab}, \mathcal{R}_\tau^{b|am}, \mathcal{R}_\tau^{a|mb}]$, where $R_\tau^{i|jk} \equiv C_{i|jk} - C_{i|j} - C_{i|k} \geqslant 0$ $(i, j, k = a, m, b)$, with $C_{u|v}$ being the contangle of a subsystem of u and v (v contains one or two modes), is a proper entanglement monotone defined as the squared logarithmic negativity. A nonzero minimum residual contangle $\mathcal{R}_\tau^{\min} > 0$ means the presence of genuine tripartite entanglement in the system.

IV. NONRECIPROCAL ENTANGLEMENT WITH KERR EFFECT

Before starting, we first point out that nonreciprocal entanglement induced by the magnon Kerr effect is different from the mechanism of the Sagnac effect. This is due to the fact that, the magnetic field mediated Kerr effect not only gives a redshift (blueshift) in magnon frequency, but also generates a two-magnon effect. To study nonreciprocal entanglement, the following experimentally accessible parameters are used: $\omega_a = \omega_m = 2\pi \times 10$ GHz, $\omega_b/2\pi = 10$ MHz, $\kappa_a/2\pi = \gamma_m/2\pi = 0.4\omega_b$, $\gamma_b/2\pi = 100$ Hz, $g_m = g_b = 2\pi \times 0.5\omega_b$, $K = \kappa_a$, $T = 10$ mK, $\tilde{\Delta}_a = \omega_b$, and $\Delta_m = -\omega_b$. These parameters numerically guarantee the system stability according to the Routh-Hurwitz criterion [76]. To investigate nonreciprocal entanglements, we plot three logarithmic negativities and the minimum residual contangle versus the magnon frequency detuning Δ_m in Fig. 2. The red and blue curves respectively denote the magnetic field along the crystalline axis [100] and [110], corresponding to $\Delta_K > 0$ and $\Delta_K < 0$. For comparison, entanglement without the Kerr effect (i.e., $\Delta_K = 0$) is also presented (see the green curve in Fig. 2). From Fig. 2(a), we can see that the optomechanical entanglement E_{ab} decreases first and then increases with Δ_m in the absence of the Kerr effect (see the green curve), while magnon-photon (E_{am})
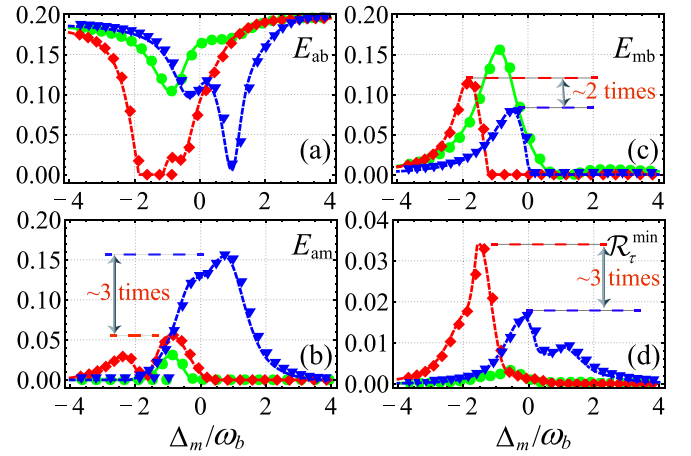

FIG. 2. Logarithmic negativities (a) E_{ab}, (b) E_{am}, (c) E_{mb}, and (d) the minimum residual contangle $\mathcal{R}_\tau^{\min}$, vs magnon frequency detuning Δ_m with $\Delta_K > 0$ (the red curve), $\Delta_K = 0$ (the green curve), and $\Delta_K < 0$ (the blue curve). The parameters are $\omega_a = \omega_m = 2\pi \times 10$ GHz, $\omega_b/2\pi = 10$ MHz, $\kappa_a/2\pi = \gamma_m/2\pi = 0.4\omega_b$, $\gamma_b/2\pi = 100$ Hz, $g_m = g_b = 2\pi \times 0.5\omega_b$, $K = \kappa_a$, $T = 10$ mK, and $\tilde{\Delta}_a = \omega_b$.

and magnon-phonon (E_{mb}) entanglements increase first and then decrease [see Figs. 2(b) and 2(c)], which is fully opposite to E_{ab}. This indicates that the initial magnon-phonon entanglement is partially transferred to the cavity-magnon and cavity-phonon subsystems, owing to the mediation of photons. Besides, a *genuinely* tripartite entanglement is generated around $\Delta_m \approx -\omega_b$, as demonstrated by the nonzero minimum residual contangle $\mathcal{R}_\tau^{\min}$ in Fig. 2(d). When the Kerr effect is taken into account, both E_{ab} and E_{mb} have a certain reduction, but E_{am} and $\mathcal{R}_\tau^{\min}$ are enhanced. By tuning the direction of the magnetic field, i.e., changing $\Delta_K > 0$ (<0) to $\Delta_K < 0$ (>0), all entanglements have different responses (see red and blue curves in Fig. 2), corresponding to the nonreciprocity. Utilizing this nonreciprocity, magnon-phonon, magnon-photon, and magnon-photon-phonon entanglements can be enhanced by ~2, 3, and 3 times, respectively.

We also plot all entanglements versus the effective Kerr strength K in Fig. 3 to investigate the effects of the Kerr nonlinearity and the magnetic field direction on entanglements. The parameters are the same as those in Fig. 2 but $\Delta_m = -\omega_b$. From Fig. 3(a), we can see that E_{ab} nearly has a linear dependence on the strength of the Kerr effect for both $\Delta_K > 0$ and $\Delta_K < 0$. But it monotonously decreases (increases) when $\Delta_K > 0$ (<0). Figure 3(b) shows that E_{am} is nonlinearly dependent on K. Specifically, E_{am} first decreases (increases) and then increases (decreases) when $\Delta_K > 0$ (< 0). For E_{mb} in Fig. 3(c), we find it is linearly dependent on K when $\Delta_K < 0$, but when $\Delta_K > 0$, the dependence becomes nonlinear (see the blue solid curve), that is, E_{mb} decreases slowly when $\Delta_K > 0$ than the case of $\Delta_K < 0$ first, then the situation becomes opposite passing through the cross-point. For $\mathcal{R}_\tau^{\min}$ in Fig. 3(d), we can see that it is nearly unchanged with K for $\Delta_K < 0$, but sharply increases to the maximal value and then decreases for $\Delta_K < 0$. These results indicates that all entanglements can be nonreciprocally enhanced with the Kerr effect.
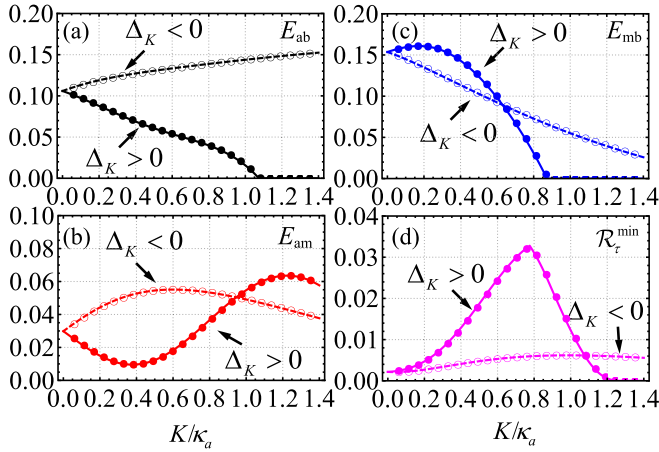
FIG. 3. Logarithmic negativities (a) E_{ab}, (b) E_{am}, (c) E_{mb}, and (d) the minimum residual contangle $\mathcal{R}_\tau^{\min}$, vs the effective Kerr strength K with $\Delta_K > 0$ and $\Delta_K < 0$. The solid circles in [(a)–(d)] denote $\Delta_K > 0$, and the open circles denote $\Delta_K < 0$. Other parameters are the same as in Fig. 2 except for $\Delta_m/\omega_b = -1$.

V. SWITCHABLE NONRECIPROCITY

In order to quantitatively describe nonreciprocal entanglement, we introduce the bidirectional contrast ratio $\mathcal{C}$ (satisfying $0 \leqslant \mathcal{C} \leqslant 1$) for bipartite and tripartite entanglements in the nonreciprocal regimes,

$$\mathcal{C}_E^{ij} = \frac{|E_{ij}(>0) - E_{ij}(<0)|}{E_{ij}(>0) + E_{ij}(<0)},$$

$$\mathcal{C}_\mathcal{R} = \frac{\left|\mathcal{R}_\tau^{\min}(>0) - \mathcal{R}_\tau^{\min}(<0)\right|}{\mathcal{R}_\tau^{\min}(>0) + \mathcal{R}_\tau^{\min}(<0)}, \quad (5)$$

where $\mathcal{C}_E^{ij}$ ($\mathcal{C}_\mathcal{R}$) = 1 and 0 correspond to the ideal and no nonreciprocities for bipartite (tripartite) entanglements. The higher is the contrast ratio $\mathcal{C}$, the stronger is the nonreciprocity of entanglement. To clearly show this, we numerically plot the contrast ratio $\mathcal{C}$ versus the frequency detuning (Δ_m) in Fig. 4(a), where the black, red, blue, and green curves respectively denote the bidirectional contrast ratios $\mathcal{C}_E^{ab}$, $\mathcal{C}_E^{am}$, $\mathcal{C}_E^{mb}$, and $\mathcal{C}_\mathcal{R}$. Obviously, the nonreciprocity of all bipartite and tripartite entanglements can be switched off and on by tuning Δ_m for $K = \kappa_a$. Moreover, the bidirectional contrast ratios for all entanglements can be tuned from 0 to 1 by varying Δ_m. This indicates that all entanglements with ideal nonreciprocity can be achieved in our proposal, via tuning the magnon frequency detuning. In Fig. 4(b), we further study the effect of Kerr strength K on the bidirectional contrast ratios at $\Delta_m = -\omega_b$. It is clearly shown that all entanglements are reciprocal in the absence of the Kerr effect, i.e., $K = 0$. When the Kerr effect is considered, all entanglements become nonreciprocal, even for the weak Kerr effect (e.g., $K = 0.2\kappa_a$). For the strong Kerr effect (e.g., $K = 1.2\kappa_a$), the bidirectional contrast ratios $\mathcal{C}_E^{ab} = \mathcal{C}_E^{am} = \mathcal{C}_\mathcal{R} = 1$ can be obtained, while $\mathcal{C}_E^{ab} < 1$ in the whole region. This shows that the nonreciprocities of the bipartite entanglements including magnon-photon and magnon-phonon entanglements and the genuinely tripartite entanglements can have ideal nonreciprocities via tuning the strength of the effective Kerr effect. Similar to the case of
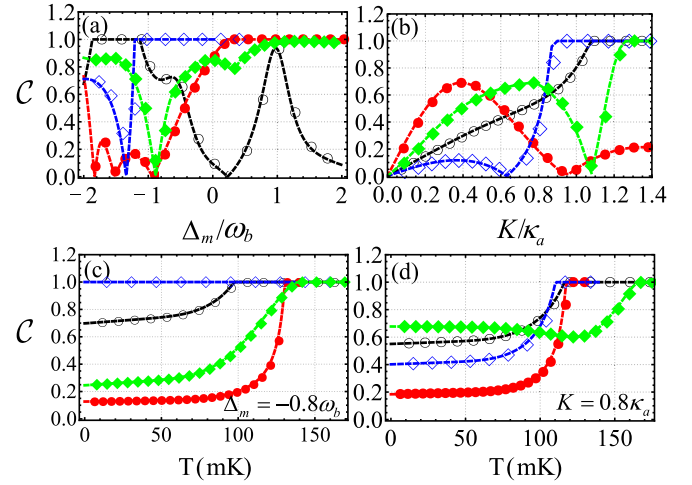

FIG. 4. (a) Bidirectional contrast ratio $\mathcal{C}$ for three bipartite and tripartite entanglements as functions of (a) magnon frequency detuning Δ_m and (b) the effective strength K. The parameters are the same as those in Fig. 2.

tuning Δ_m, the nonreciprocities for all entanglements can also be switched off and on with the Kerr effect. In addition, we examine the effect of temperature on the bidirectional contrast ratios with different parameters in Figs. 4(c) and 4(d). We find the nonreciprocity of the magnon-phonon entanglement is robust against the temperature when $\Delta_m = -0.8\omega_b$ and $K = \kappa_a$ [see the blue curve in Fig. 4(c)], while nonreciprocities of other entanglements increase slowly first with T. By further increasing T, a sharp increase occurs and the ideal nonreciprocal photon-phonon, magnon-photon, and magnon-photon-phonon entanglements can be achieved [see the other curves in Fig. 4(c)]. When $\Delta_m = -\omega_b$ and $K = 0.8\kappa_a$ [see the curves in Fig. 4(d)], one can see that nonreciprocities of all entanglements have similar behaviors with the case of the magnon-photon entanglement in Fig. 4(c). The findings suggest that a higher temperature is beneficial to obtain the large or optimal nonreciprocity for entanglement, providing another promising path to engineer the nonreciprocity.

VI. CONCLUSION

We have proposed a scheme to realize nonreciprocal entanglements with the magnon Kerr effect among magnons, photons, and phonons in a hybrid cavity-magnon optomechanical system. By applying a strong driving field on the cavity, the Kerr effect gives rise to a positive (negative) frequency shift in the magnon frequency and an additional two-magnon effect. The signs of the frequency shift and the coefficient of the two-magnon effect are dependent on the direction of the applied magnetic field, leading to nonreciprocal entanglements. By further tuning the system parameters, such as the magnon frequency detuning and strength of the Kerr effect, we find entanglements among magnons, photons, and phonons can be nonreciprocally enhanced via changing the direction of the magnetic field. We also show that entanglement nonreciprocity in our proposal, characterized by the defined bidirectional contrast ratio, can be switched off and on by tuning the system parameters. With proper parameters, ideal nonreciprocal entanglements can be achieved. Finally, we find

that nonreciprocity can be improved with the bath temperature, even to the ideal value. The results suggest that our scheme provides an alternative path to realize nonreciprocal entanglement with the Kerr effect and engineer nonreciprocity with the bath temperature.

ACKNOWLEDGMENT

APPENDIX

In this Appendix, we give a detailed derivation of the effective Hamiltonian (1) and the drift matrix A given by Eq. (3) in the main text.

We consider a hybrid cavity-magnon optomechanical system consisting of a driven cavity simultaneously coupled to a micron-sized yttrium iron garnet (YIG) sphere and a mechanical resonator. The Hamiltonian of the total system can be written as (setting $\hbar = 1$)

$$H = H_{om} + H_{kerr} + H_{int} + H_d, \tag{A1}$$

with

$$
\begin{aligned}
H_{om} &= \omega_a a^\dagger a + \tfrac{1}{2}\omega_b(p^2 + q^2) - g_0 a^\dagger a q, \\
H_{kerr} &= \omega_m m^\dagger m + K_0 (m^\dagger m)^2 \\
H_{int} &= g_m(a^\dagger m + a m^\dagger) \\
H_d &= i\Omega_0\big(a^\dagger e^{-i\omega_0 t} - a e^{i\omega_0 t}\big). \tag{A2}
\end{aligned}
$$

Using a unitary transformation $R = \exp[-i\omega_0(a^\dagger a + m^\dagger m)t]$, we can change the system's operators as $a \to a \exp(-i\omega_0 t)$, $a^\dagger \to a^\dagger \exp(i\omega_0 t)$, $m \to m \exp(-i\omega_0 t)$, and $m^\dagger \to m^\dagger \exp(i\omega_0 t)$. Thus,

$$
\begin{aligned}
H_{om} &\to (\omega_a - \omega_0)a^\dagger a + \tfrac{1}{2}\omega_b(p^2 + q^2) - g_0 a^\dagger a q, \\
H_{kerr} &\to \Delta_m m^\dagger m + K_0(m^\dagger m)^2, \tag{A3} \\
H_{int} &\to H_{int}, \quad H_D \to i\Omega_0(a^\dagger - a),
\end{aligned}
$$

where $\Delta_m = \omega_m - \omega_0$.

With the Heisenberg-Langevin approach, the quantum dynamics of the considered system can be governed by the following quantum Langevin equations,

$$
\begin{aligned}
\dot{q} &= \omega_b p, \\
\dot{p} &= -\omega_b q + g_0 a^\dagger a - \gamma_b p + \xi, \\
\dot{a} &= -[i(\omega_a - \omega_0) + \kappa_a]a + ig_0 a q - ig_m m + \Omega_0 + \sqrt{2\kappa_a}a_{in}, \\
\dot{m} &= -(i\Delta_m + \gamma_m)m - ig_m a - iK_0 m^\dagger m m + \sqrt{2\gamma_m}m_{in}, \tag{A4}
\end{aligned}
$$

where κ_a and γ_m are the decay rates of the cavity and mechanical modes, respectively. a_{in}, m_{in}, and ξ are the input noise operators with zero-mean value (i.e., $\langle a_{in}\rangle = \langle m_{in}\rangle = \langle\xi\rangle = 0$).

Below we employ the standard linearization method [12] to derive the linearized Hamiltonian in Eq. (1) (see the main

text). We rewrite each operator as the sum of the mean value (i.e., operator expectation) and the corresponding fluctuation, i.e.,

$$q \to q_s + q, \quad p \to p_s + p, \quad a \to a_s + a, \quad m \to m_s + m. \tag{A5}$$

Substituting Eq. (A5) into Eq. (A4), we can obtain the following equations for the mean values of the operators,

$$
\begin{aligned}
\dot{q}_s &= \omega_b p_s, \quad \dot{p}_s = -\omega_b q_s + g_0|a_s|^2 - \gamma_b p_s, \\
\dot{a}_s &= -(i\tilde{\Delta}_a + \kappa_a)a_s - ig_m m_s + \Omega_0, \tag{A6} \\
\dot{m}_s &= -(i\tilde{\Delta}_m + \gamma_m)m_s - ig_m a_s,
\end{aligned}
$$

where $\tilde{\Delta}_a = \omega_a - \omega_0 - g_0 q_s$ is the effective cavity frequency detuning induced by the displacement of the mechanical resonator, and $\tilde{\Delta}_m = \Delta_m + \Delta_K$ with $\Delta_K = 2K = 4K_0 N_m = 4K_0|m_s|^2$ is the effective magnon frequency detuning induced by the Kerr effect. In the long-time limit, $\dot{q}_s = \dot{p}_s = \dot{a}_s = \dot{m}_s = 0$. The steady-state condition directly gives

$$
\begin{aligned}
p_s &= 0, \quad q_s = g_0|a_s|^2/\omega_b, \\
m_s &= -ig_m a_s/(i\tilde{\Delta}_m + \gamma_m), \tag{A7} \\
a_s &= (\Omega_0 - ig_m m_s)/(i\tilde{\Delta}_a + \kappa_a).
\end{aligned}
$$

Also, the equations for the quantum fluctuations, which are obtained by substituting Eq. (A5) into Eq. (A4) and neglecting high-order fluctuation terms, are given by

$$
\begin{aligned}
\dot{q} &= \omega_b p, \quad \dot{p} = -\omega_b q + g_b(a + a^\dagger)/\sqrt{2} - \gamma_b p + \xi, \\
\dot{a} &= -(i\tilde{\Delta}_a + \kappa_a)a + ig_b q/\sqrt{2} - ig_m m + \sqrt{2\kappa_a}a_{in}, \tag{A8} \\
\dot{m} &= -(i\tilde{\Delta}_m + \gamma_m)m - ig_m a - iKm^\dagger + \sqrt{2\gamma_m}m_{in},
\end{aligned}
$$

where $g_b = \sqrt{2}g_0 a_s$ is the enhanced linearized optomechanical coupling via tuning the strong driving field. Obviously, Eq. (A8) is the same as Eq. (2) in the main text. The corresponding linearized Hamiltonian of the hybrid system without dissipation can be written as

$$
\begin{aligned}
\mathcal{H} &= \tilde{\Delta}_a a^\dagger a + \tilde{\Delta}_m m^\dagger m + \frac{1}{2}\omega_b(q^2 + p^2) - \frac{1}{\sqrt{2}}g_b(a + a^\dagger)q \\
&\quad + g_m(a^\dagger m + a m^\dagger) + \frac{1}{2}K(m^{\dagger 2} + m^2), \tag{A9}
\end{aligned}
$$

which is just Eq. (1) in the main text.

By further defining quadratures,

$$
\begin{aligned}
x_a(t) &= \frac{a + a^\dagger}{\sqrt{2}}, \quad y_a(t) = \frac{a - a^\dagger}{i\sqrt{2}}, \\
x_m(t) &= \frac{m + m^\dagger}{\sqrt{2}}, \quad y_m(t) = \frac{m - m^\dagger}{i\sqrt{2}}, \tag{A10}
\end{aligned}
$$

Equation (A8) can be rewritten as

$$
\begin{aligned}
\dot{q} &= \omega_b p, \quad \dot{p} = -\omega_b q + g_b x_a - \gamma_b p + \xi, \\
\dot{x}_a &= -\kappa_a x_a + \tilde{\Delta}_a + g_m y_m + \sqrt{2\kappa_a}x_{in}^a(t), \\
\dot{y}_a &= -\tilde{\Delta}_a x_a - \kappa_a y_a - g_m x_m + \sqrt{2\kappa_a}y_{in}^a(t), \tag{A11} \\
\dot{x}_m &= -\gamma_m x_a + \tilde{\Delta}_m^- y_m + g_m y_a + \sqrt{2\gamma_m}x_{in}^m(t), \\
\dot{y}_m &= -\tilde{\Delta}_m^+ x_m - \gamma_m y_m - g_m x_a + \sqrt{2\gamma_m}y_{in}^m(t),
\end{aligned}
$$

where $x_{\mathrm{in}}^a(t) = (a_{\mathrm{in}} + a_{\mathrm{in}}^\dagger)/\sqrt{2}$, $y_{\mathrm{in}}^a(t) = (a_{\mathrm{in}} - a_{\mathrm{in}}^\dagger)/i\sqrt{2}$, $x_{\mathrm{in}}^m(t) = (m_{\mathrm{in}} + m_{\mathrm{in}}^\dagger)/\sqrt{2}$, and $y_{\mathrm{in}}^m(t) = (m_{\mathrm{in}} - m_{\mathrm{in}}^\dagger)/i\sqrt{2}$. Here, $\tilde{\Delta}_m^\pm = \tilde{\Delta}_m \pm \Delta_K/2$. In compact form, Eq. (A11) can be given by

$$\dot{u}(t) = Au(t) + f(t), \tag{A12}$$

where $u(t) = [x_a(t), y_a(t), x_m(t), y_m(t), q(t), p(t)]^T$ and $f(t) = [\sqrt{2\kappa_a} x_{\mathrm{in}}^a(t), \sqrt{2\kappa_a} y_{\mathrm{in}}^a(t), \sqrt{2\gamma_m} x_{\mathrm{in}}^m(t), \sqrt{2\gamma_m} y_{\mathrm{in}}^m(t), 0, \xi(t)]^T$ are the vectors of the system and the input noise operators, respectively, and the drift (coefficient) matrix A is given by Eq. (3) in the main text.

---

[1] D. Bouwmeester, A. Ekert, and A. Zeilinger, *The Physics of Quantum Information* (Springer, Berlin, 2000).

[2] S. Haroche, Entanglement, decoherence and the quantum/classical boundary, Phys. Today **51**(7), 36 (1998).

[3] M. Aspelmeyer, T. J. Kippenberg, and F. Marquardt, Cavity optomechanics, Rev. Mod. Phys. **86**, 1391 (2014).

[4] W. Xiong, J. Chen, B. Fang, M. Wang, L. Ye, and J. Q. You, Strong tunable spin-spin interaction in a weakly coupled nitrogen vacancy spin-cavity electromechanical system, Phys. Rev. B **103**, 174106 (2021).

[5] X.-Y. Lü, W. M. Zhang, S. Ashhab, Y. Wu, and F. Nori, Quantum-criticality-induced strong Kerr nonlinearities in optomechanical systems, Sci. Rep. **3**, 2943 (2013).

[6] J. Chen, Z. Li, X. Q. Luo, W. Xiong, M. Wang, and H. C. Li, Strong single-photon optomechanical coupling in a hybrid quantum system, Opt. Express **29**, 32639 (2021).

[7] W. Xiong, M. Wang, G. Q. Zhang, and J. Chen, Optomechanical-interface-induced strong spin-magnon coupling, Phys. Rev. A **107**, 033516 (2023).

[8] W. Xiong, D. Y. Jin, Y. Qiu, C. H. Lam, and J. Q. You, Cross-Kerr effect on an optomechanical system, Phys. Rev. A **93**, 023844 (2016).

[9] X. Y. Lü, H. Jing, J. Y. Ma, and Y. Wu, $\mathcal{PT}$-Symmetry Breaking Chaos in Optomechanics, Phys. Rev. Lett. **114**, 253601 (2015).

[10] W. Xiong, Z. Li, Y. Song, J. Chen, G. Q. Zhang, and M. Wang, Higher-order exceptional point in a pseudo-Hermitian cavity optomechanical system, Phys. Rev. A **104**, 063508 (2021).

[11] W. Xiong, Z. Li, G. Q. Zhang, M. Wang, H. C. Li, X. Q. Luo, and J. Chen, Higher-order exceptional point in a blue-detuned non-Hermitian cavity optomechanical system, Phys. Rev. A **106**, 033518 (2022).

[12] D. Vitali, S. Gigan, A. Ferreira, H. R. Böhm, P. Tombesi, A. Guerreiro, V. Vedral, A. Zeilinger, and M. Aspelmeyer, Optomechanical Entanglement between a Movable Mirror and a Cavity Field, Phys. Rev. Lett. **98**, 030405 (2007).

[13] L. Tian, Robust Photon Entanglement via Quantum Interference in Optomechanical Interfaces, Phys. Rev. Lett. **110**, 233602 (2013).

[14] Y. D. Wang and A. A. Clerk, Reservoir-Engineered Entanglement in Optomechanical Systems, Phys. Rev. Lett. **110**, 253601 (2013).

[15] S. Mancini, V. Giovannetti, D. Vitali, and P. Tombesi, Entangling Macroscopic Oscillators Exploiting Radiation Pressure, Phys. Rev. Lett. **88**, 120401 (2002).

[16] D. G. Lai, J. Q. Liao, A. Miranowicz, and F. Nori, Noise-Tolerant Optomechanical Entanglement via Synthetic Magnetism, Phys. Rev. Lett. **129**, 063602 (2022).

[17] T. A. Palomaki, J. D. Teufel, R. W. Simmonds, and K. W. Lehnert, Entangling mechanical motion with microwave fields, Science **342**, 710 (2013).

[18] C. F. Ockeloen-Korppi, E. Damskägg, J. M. Pirkkalainen, A. A. Clerk, F. Massel, M. J. Woolley, and M. A. Sillanpää, Stabilized entanglement of massive mechanical oscillators, Nature (London) **556**, 478 (2018).

[19] S. Kotler, G. A. Peterson, E. Shojaee, F. Lecocq, K. Cicak, A. Kwiatkowski, S. Geller, S. Glancy, E. Knill, R. W. Simmonds, J. Aumentado, and J. D. Teufel, Direct observation of deterministic macroscopic entanglement, Science **372**, 622 (2021).

[20] L. Mercier de Lépinay, C. F. Ockeloen-Korppi, M. J. Woolley, and M. A. Sillanpää, Quantum mechanics-free subsystem with mechanical oscillators, Science **372**, 625 (2021).

[21] R. Riedinger, A. Wallucks, I. Marinkovic, C. Löschnauer, M. Aspelmeyer, S. Hong, and S. Gröblacher, Remote quantum entanglement between two micromechanical oscillators, Nature (London) **556**, 473 (2018).

[22] Y. F. Jiao, S. D. Zhang, Y. L. Zhang, A. Miranowicz, L. M. Kuang, and H. Jing, Nonreciprocal Optomechanical Entanglement against Backscattering Losses, Phys. Rev. Lett. **125**, 143605 (2020).

[23] Y. F. Jiao, J. X. Liu, Y. Li, R. Yang, L. M. Kuang, and H. Jing, Nonreciprocal Enhancement of Remote Entanglement between Nonidentical Mechanical Oscillators, Phys. Rev. Appl. **18**, 064008 (2022).

[24] H. Xu, L. Jiang, A. A. Clerk, and J. G. E. Harris, Nonreciprocal control and cooling of phonon modes in an optomechanical system, Nature (London) **568**, 65 (2019).

[25] Z. Shen, Y. L. Zhang, Y. Chen, C. L. Zou, Y. F. Xiao, X. B. Zou, F. W. Sun, G. C. Guo, and C. H. Dong, Experimental realization of optomechanically induced non-reciprocity, Nat. Photon. **10**, 657 (2016).

[26] D. W. Zhang, L. L. Zheng, C. You, C. S. Hu, Y. Wu, and X. Y. Lü, Nonreciprocal chaos in a spinning optomechanical resonator, Phys. Rev. A **104**, 033522 (2021).

[27] X. Y. Yao, H. Ali, F. L. Li, and P. B. Li, Nonreciprocal Phonon Blockade in a Spinning Acoustic Ring Cavity Coupled to a Two-Level System, Phys. Rev. Appl. **17**, 054004 (2022).

[28] Y. Jiang, S. Maayani, T. Carmon, F. Nori, and H. Jing, Nonreciprocal Phonon Laser, Phys. Rev. Appl. **10**, 064037 (2018).

[29] M. Peng, H. Zhang, Q. Zhang, T. X. Lu, I. M. Mirza, and H. Jing, Nonreciprocal slow or fast light in anti-$\mathcal{PT}$-symmetric optomechanics, Phys. Rev. A **107**, 033507 (2023).

[30] H. Xie, L. W. He, X. Shang, G. W. Lin, and X. M. Lin, Nonreciprocal photon blockade in cavity optomagnonics, Phys. Rev. A **106**, 053707 (2022).

[31] W. A. Li, G. Y. Huang, J. P. Chen, and Y. Chen, Nonreciprocal enhancement of optomechanical second-order sidebands in a spinning resonator, Phys. Rev. A **102**, 033526 (2020).

[32] G. B. Malykin, The Sagnac effect: Correct and incorrect explanations, Phys. Usp. **43**, 1229 (2000).

[33] S. Maayani, R. Dahan, Y. Kligerman, E. Moses, A. U. Hassan, H. Jing, F. Nori, D. N. Christodoulides, and T. Carmon, Flying couplers above spinning resonators generate irreversible refraction, Nature (London) **558**, 569 (2018).

[34] B. Z. Rameshti, S. V. Kusminskiy, J. A. Haigh, K. Usami, D. Lachance-Quirion, Y. Nakamura, C. M. Hu, H. X. Tang, G. E. W. Bauer, and Y. M. Blanter, Cavity magnonics, Phys. Rep. **979**, 1 (2022).

[35] H. Y. Yuan, Y. Cao, A. Kamra, R. A. Duine, and P. Yan, Quantum magnonics: When magnon spintronics meets quantum information science, Phys. Rep. **965**, 1 (2022).

[36] D. Lachance-Quirion, Y. Tabuchi, A. Gloppe, K. Usami, and Y. Nakamura, Hybrid quantum systems based on magnonics, Appl. Phys. Express **12**, 070101 (2019).

[37] Y. P. Wang and C.-M. Hu, Dissipative couplings in cavity magnonics, J. Appl. Phys. **127**, 130901 (2020).

[38] S. Zheng, Z. Wang, Y. Wang, F. Sun, Q. He, P. Yan, and H. Y. Yuan, Tutorial: Nonlinear magnonics, arXiv:2303.16313.

[39] J. Li, S. Y. Zhu, and G. S. Agarwal, Magnon-Photon-Phonon Entanglement in Cavity Magnomechanics, Phys. Rev. Lett. **121**, 203601 (2018).

[40] M. Yu, H. Shen, and J. Li, Magnetostrictively Induced Stationary Entanglement between Two Microwave Fields, Phys. Rev. Lett. **124**, 213604 (2020).

[41] Z. Zhang, M. O. Scully, and G. S. Agarwal, Quantum entanglement between two magnon modes via Kerr nonlinearity driven far from equilibrium, Phys. Rev. Res. **1**, 023021 (2019).

[42] R. C. Shen, J. Li, Z. Y. Fan, Y. P. Wang, and J. Q. You, Mechanical Bistability in Kerr-modified Cavity Magnomechanics, Phys. Rev. Lett. **129**, 123601 (2022).

[43] R. C. Shen, Y. P. Wang, J. Li, S. Y. Zhu, G. S. Agarwal, and J. Q. You, Long-Time Memory and Ternary Logic Gate Using a Multistable Cavity Magnonic System, Phys. Rev. Lett. **127**, 183202 (2021).

[44] Y. P. Wang, G. Q. Zhang, D. Zhang, T. F. Li, C. M. Hu, and J. Q. You, Bistability of Cavity Magnon Polaritons, Phys. Rev. Lett. **120**, 057202 (2018).

[45] Y. P. Wang, G. Q. Zhang, D. Zhang, X. Q. Luo, W. Xiong, S. P. Wang, T. F. Li, C. M. Hu, and J. Q. You, Magnon Kerr effect in a strongly coupled cavity-magnon system, Phys. Rev. B **94**, 224410 (2016).

[46] G. Q. Zhang, Y. P. Wang, and J. Q. You, Theory of the magnon Kerr effect in cavity magnonics, Sci. China: Phys. Mech. Astron. **62**, 987511 (2019).

[47] W. Xiong, M. Tian, G. Q. Zhang, and J. Q. You, Strong long-range spin-spin coupling via a Kerr magnon interface, Phys. Rev. B **105**, 245310 (2022).

[48] G. Q. Zhang, Z. Chen, W. Xiong, C. H. Lam, and J. Q. You, Parity-symmetry-breaking quantum phase transition in a cavity magnonic system driven by a parametric field, Phys. Rev. B **104**, 064423 (2021).

[49] G. Liu, W. Xiong, and Z. J. Ying, Switchable superradiant phase transition with Kerr magnons, arXiv:2302.07163.

[50] G. Q. Zhang, Y. Wang, and W. Xiong, Detection sensitivity enhancement of magnon Kerr nonlinearity in cavity magnonics induced by coherent perfect absorption, Phys. Rev. B **107**, 064417 (2023).

[51] T. Tian, Y. Zhang, L. Zhang, L. Wu, S. Lin, J. Zhou, C. K. Duan, J. H. Jiang, and J. Du, Experimental Realization of Nonreciprocal Adiabatic Transfer of Phonons in a Dynamically Modulated Nanomechanical Topological Insulator, Phys. Rev. Lett. **129**, 215901 (2022).

[52] C. Zhong, X. Han, and L. Jiang, Microwave and Optical Entanglement for Quantum Transduction with Electro-Optomechanics, Phys. Rev. Appl. **18**, 054061 (2022).

[53] J. I. Cirac, P. Zoller, H. J. Kimble, and H. Mabuchi, Quantum State Transfer and Entanglement Distribution among Distant Nodes in a Quantum Network, Phys. Rev. Lett. **78**, 3221 (1997).

[54] J. Kimble, The quantum internet, Nature (London) **453**, 1023 (2008).

[55] P. Lodahl, S. Mahmoodian, S. Stobbe, A. Rauschenbeutel, P. Schneeweiss, J. Volz, H. Pichler, and P. Zoller, Chiral quantum optics, Nature (London) **541**, 473 (2017).

[56] C. Gonzalez-Ballestero, A. Gonzalez-Tudela, F. J. GarciaVidal, and E. Moreno, Chiral route to spontaneous entanglement generation, Phys. Rev. B **92**, 155304 (2015).

[57] S. A. H. Gangaraj, G. W. Hanson, and M. Antezza, Robust-tentanglement with three-dimensional nonreciprocal photonic topological insulators, Phys. Rev. A **95**, 063807 (2017).

[58] G. Hu, X. Hong, K. Wang, J. Wu, H. X. Xu, W. Zhao, W. Liu, S. Zhang, F. Garcia-Vidal, B. Wang, P. Lu, and C. W. Qiu, Coherent steering of nonlinear chiral valley photons with a synthetic Au-WS$_2$ metasurface, Nat. Photon. **13**, 467 (2019).

[59] C. L. Degen, F. Reinhard, and P. Cappellaro, Quantum sensing, Rev. Mod. Phys. **89**, 035002 (2017).

[60] I. Marinković, A. Wallucks, R. Riedinger, S. Hong, M. Aspelmeyer, and S. Gröblacher, Optomechanical Bell Test, Phys. Rev. Lett. **121**, 220404 (2018).

[61] S. G. Hofer and K. Hammerer, Entanglement-enhanced time-continuous quantum control in optomechanics, Phys. Rev. A **91**, 033822 (2015).

[62] S. Barzanjeh, M. Abdi, G. J. Milburn, P. Tombesi, and D. Vitali, Reversible Optical-to-Microwave Quantum Interface, Phys. Rev. Lett. **109**, 130503 (2012).

[63] S. G. Hofer, W. Wieczorek, M. Aspelmeyer, and K. Hammerer, Quantum entanglement and teleportation in pulsed cavity-optomechanics, Phys. Rev. A **84**, 052327 (2011).

[64] X. W. Xu, Y. Li, A. X. Chen, and Y. Liu, Nonreciprocal conversion between microwave and optical photons in electro-optomechanical systems, Phys. Rev. A **93**, 023827 (2016).

[65] L. Tian and Z. Li, Nonreciprocal quantum-state conversion between microwave and optical photons, Phys. Rev. A **96**, 013808 (2017).

[66] N. Eshaqi-Sani, S. Zippilli, and D. Vitali, Nonreciprocal conversion between radio-frequency and optical photons with an optoelectromechanical system, Phys. Rev. A **106**, 032606 (2022).

[67] Y. L. Ren, Nonreciprocal optical-microwave entanglement in a spinning magnetic resonator, Opt. Lett. **47**, 1125 (2022).

[68] K. Stannigel, P. Komar, S. J. M. Habraken, S. D. Bennett, M. D. Lukin, P. Zoller, and P. Rabl, Optomechanical Quantum Information Processing with Photons and Phonons, Phys. Rev. Lett. **109**, 013603 (2012).

[69] R. Horodecki, P. Horodecki, M. Horodecki, and K. Horodecki, Quantum entanglement, Rev. Mod. Phys. **81**, 865 (2009).

[70] U. L. Andersen, G. Leuchs, and C. Silberhorn, Continuous variable quantum information processing, Laser Photonics Rev. **4**, 337 (2010).

[71] S. L. Braunstein and P. van Loock, Quantum information with continuous variables, Rev. Mod. Phys. **77**, 513 (2005).

[72] D. F. Walls and G. J. Milburn, *Quantum Optics* (Springer, Berlin, 1994).

[73] G. Vidal and R. F. Werner, Computable measure of entanglement, Phys. Rev. A **65**, 032314 (2002).

[74] M. B. Plenio, Logarithmic Negativity: A Full Entanglement Monotone That is not Convex, Phys. Rev. Lett. **95**, 090503 (2005).

[75] G. Adesso and F. Illuminati, Continuous variable tangle, monogamy inequality, and entanglement sharing in Gaussian states of continuous variable systems, New J. Phys. **8**, 15 (2006).

[76] I. S. Gradshteyn and I. M. Ryzhik, *Table of Integrals, Series and Products* (Academic, Orlando, Florida, 1980).